

## Evolution of nanoscale morphology on fracture surface of brittle metallic glass

G. Wang, Y. T. Wang, Y. H. Liu, M. X. Pan, D. Q. Zhao, and W. H. Wang<sup>a)</sup>  
*Institute of Physics, Chinese Academy of Sciences, Beijing 100080, People's Republic of China*

(Received 11 April 2006; accepted 1 August 2006; published online 19 September 2006)

The authors report the observations of periodic morphology evolution on fracture surface of a brittle metallic glassy ribbon, suggesting a wavy local stress intensity factor along the crack propagation. The authors find that the formation of nanoscale damage cavity structure is a common characteristic morphology on the fracture surfaces. On the surface of the hackle zone, these cavities assemble and generate the nanoscale swirling periodic corrugations. The elastic waves interfering with the plastic process zone on the crack front is proposed to explain such dynamic crack instability. The authors' observations support the notion of an impinging effect of elastic waves on propagating crack front. © 2006 American Institute of Physics. [DOI: 10.1063/1.2354011]

Dynamic crack propagation is an inevitable phenomenon during the fracture process in most materials, which is a basic problem for understanding the damage behavior of engineering materials.<sup>1-5</sup> The dynamic crack propagation brings out the instability in crack front due to second fracture, dynamic crack-tip field twist, oscillating, branching, and acoustic wave emission, etc.,<sup>5-10</sup> which generally generate special fractography in macroscale consisting of mirror, mist, and hackle zones. During the dynamic crack propagating process, the release of fracture energy will be transformed as fracture surface energy and acoustic emission in a form of elastic wave spreading into the bulk as shear wave and/or along the newly formed fracture surface as Rayleigh wave.<sup>9,11,12</sup> These propagating waves can interfere with stress field in the crack tip, which will generate complicated morphologies on the crack surface.<sup>13,14</sup> The morphologies are in microscale of Wallner lines and some periodic corrugations on fracture surface of brittle materials.<sup>4-6,10</sup> However, the precise physical origin of the corrugations remains unclear.<sup>14-17</sup> More experimental observations focused on a detailed understanding of the dynamic crack surface marking patterns are needed to address these fundamental points.

Fracture behavior of metallic glasses is strongly correlated with toughness. The stress intensity factor ( $K_c$ ) varies significantly among brittle metallic glasses (BMGs) from  $\sim 80 \text{ MPa m}^{1/2}$  for Pt-based BMGs to  $5 \text{ MPa m}^{1/2}$  for Mg-, Ce-, and Fe-based BMGs.<sup>18</sup> Metallic glasses normally exhibit a macroscopic brittle fracture while plastic deformation ability only appears on the crack-tip zone in micro- or even nanoscale depending on  $K_c$ .<sup>18</sup> Fracture behavior of metallic glasses is dominated by shear bands, and the shear fracture along the shear band brings out an adiabatic heating generally resulting in viscous layer on the fracture surface,<sup>19,20</sup> in which any tiny change of the local crack-tip stress field should more easily leave obvious markings on the fracture surface. In addition, comparing with nonmetallic glasses, the fracture surface features of conducting metallic glasses can be conveniently investigated on a nanoscale by high resolution scanning electron microscopy (HRSEM), providing more information at high spatial resolution about crack

propagation, which is very important for understanding the mechanism of the dynamic fracture. In this letter, the dynamic crack propagation was investigated in a  $\text{Fe}_{73.5}\text{Cu}_1\text{Nb}_3\text{Si}_{13.5}\text{B}_9$  (at. %) glassy ribbon, which is a brittle glass with  $K_c = 5 \text{ MPa m}^{1/2}$ . The nanoscale morphology and its evolution in the fracture surface of the brittle metallic glass were observed and explained.

The  $\text{Fe}_{73.5}\text{Cu}_1\text{Nb}_3\text{Si}_{13.5}\text{B}_9$  glassy ribbon with a size of  $25 \mu\text{m}$  in thickness and  $14 \text{ mm}$  in width was prepared by rapid quenching method with a cooling rate of  $10^5 \text{ K/s}$ . To remove the residual stress resulted from the rapid quenching process, the glassy ribbon was preannealed at the glass transition temperature for 10 min. A small "seed" crack was introduced at the edge of the ribbon. To initiate fracture, the glassy ribbon was stretched by applying a uniform displacement at its vertical boundaries with a moving speed of  $0.01 \text{ mm/min}$ . The crack propagation along the width direction always originates from the seed crack on the edge of the ribbon. A uniaxial tension was performed along the length direction on an Instron-type universal tester. The fractography was observed using a Philips XL 30 scanning electron microscope.

The fractography of the crack fracture surface shows a periodic morphology consisting of river-pattern, mist, and hackle zones with crack propagating, which are shown in Figs. 1(a)–1(c). The average length for the periodic morphology is measured to be  $356 \mu\text{m}$ . The river patterns appear on the region near the notch and along the crack propagating direction [see Fig. 1(a)]. The river patterns are formed due to the crack branching which also generates numerous damage cavities with the size from  $100$  to  $160 \text{ nm}$  on the valley of crack branching vein [see the inset of Fig. 1(a)]. The crack branching, which is usually regarded as the result of the high crack propagating velocity,<sup>17,18</sup> occurs near the notch in the present study. As such, the river-pattern zone is possibly dominated by the change of local stress intensity. With crack propagating, the river pattern is replaced by the mist pattern as shown in Fig. 1(b). The mist zone also contains a plenty of cavity structures [see the inset of Fig. 1(b)] while their size (from  $106$  to  $205 \text{ nm}$ ) is obviously larger than that in the river-pattern zone. When the crack further propagates to a critical stage, the crack starts to bifurcate along its front, and the river patterns reappear, but exhibit swirling flow mor-

<sup>a)</sup> Author to whom correspondence should be addressed; electronic mail: whw@aphy.iphy.ac.cn

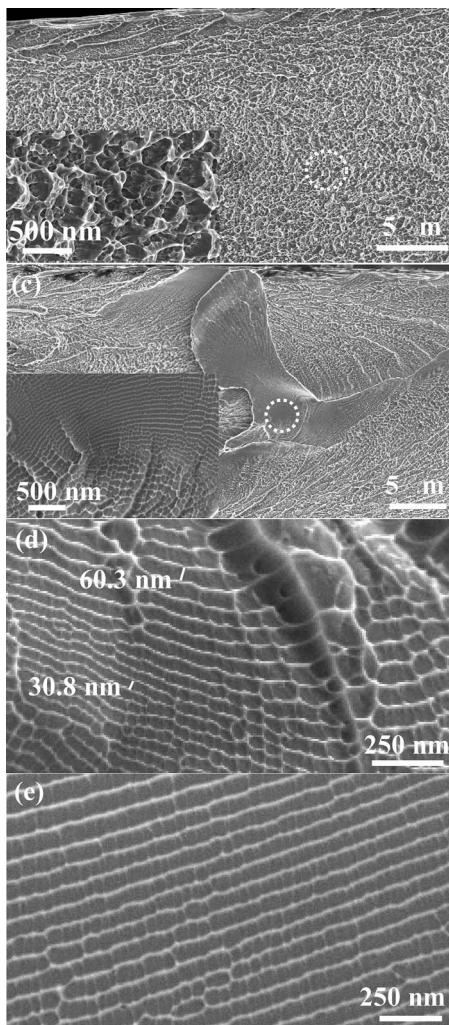


FIG. 1. Fractography of the crack surface of the  $\text{Fe}_{73.5}\text{Cu}_1\text{Nb}_3\text{Si}_{13.5}\text{B}_9$  metallic glassy ribbon (insets showing the enlarged images). (a) River-pattern zone (inset image corresponding to circle region). (b) mist zone (inset image corresponding to the circle region). (c) Hackle zone (inset image corresponding to circle region). [(d) and (e)] Periodic corrugations.

phologies that induce severe surface roughness, i.e., the hackle zone formed [see Fig. 1(c)]. A transformation region is observed in the center of the swirling river pattern [see the inset of Fig. 1(c)] where the cavities are reduced in size and arranged spirally. As the size of the cavities decreases to a critical size of about 70 nm, surprisingly, these cavities assemble and form the periodic corrugations and spread spirally to the center of the swirling pattern with the corrugation periodic length reducing from approximately 60 to 30 nm [see Fig. 1(d)]. In the center of the swirling pattern, the periodic corrugations are clearly observed [see Fig. 1(e)]. Furthermore, the parts of river patterns stretch to the next periodic morphology. Figure 2 shows a sketch of periodic morphology evolution on the fracture surface of the glassy ribbon.

The formation of damage cavity structure is a characteristic morphology in metallic glasses.<sup>21</sup> The size of cavity ( $w$ ) was associated with  $K_C$  of the metallic glass as<sup>18</sup>  $w = K_C^2 / (6\pi\sigma_Y^2)$ , where  $\sigma_Y$  is yielding stress. Since the patterns appear periodically along the crack propagating direction, we measured  $w$  of the  $\text{Fe}_{73.5}\text{Cu}_1\text{Nb}_3\text{Si}_{13.5}\text{B}_9$  metallic glass at different spots along the crack propagating direction with an interval distance of 20  $\mu\text{m}$ . The measured  $w$  and the corre-

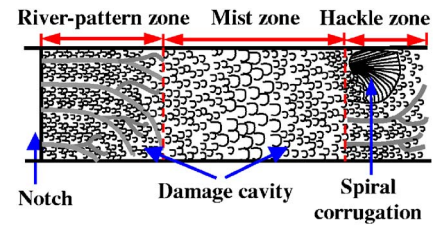


FIG. 2. (Color online) Sketch of periodic morphology evolution on the fracture surface.

sponding  $K_C$  as functions of the crack propagating distance are plotted in Fig. 3, in which two periodic morphologies are exhibited. The changes of  $w$  in the river-pattern zone (I: 100–160 nm) and the mist zone (II: 160–210 nm) can be clearly seen. A maximum value of  $w$  presents in the mist zone accompanying the maximum toughness. Since the hackle zone contains river-pattern and swirling corrugations, the values of  $w$  reduce from 160 to 30 nm (region III).

According to the linear elastic fracture mechanics (LEFM),<sup>4</sup>  $K_C \propto \sqrt{G}$ , where  $G$  is the energy flux and is defined as per unit length of the crack with the fracture energy.<sup>15</sup> For dynamic crack propagation,  $G$  depends on propagating velocity  $v$ . With crack propagating from notch to mist zone,  $v$  increases and further results in the increase of  $G$ .<sup>5</sup> As a result, the local  $K_C$  increases from approximately 4.5  $\text{MPa m}^{1/2}$  in the river-pattern zone to 6.3  $\text{MPa m}^{1/2}$  in the mist zone (see Fig. 3). When  $v$  is further increased, the crack starts to bifurcate along its front to dissipate the increased kinetic energy of the fast running crack and produces fracture surface distortion in hackle zone and more fracture surfaces [see Fig. 1(c)].<sup>10,22</sup> The formation of hackle zone can reduce the value of  $K_C$ ,<sup>10</sup> which is consistent with the results shown in Fig. 3. When the  $K_C$  is further reduced, the river patterns reappear in the hackle zone and stretch to the next periodic morphology, and another periodicity of crack propagation process commences.

However, the formation and evolution of the nanoscale cavities observed in this brittle glass cannot be explained by the LEFM, because in this scale elastic stress wave has become another dominating factor for the surface roughness,<sup>9</sup> which shows the coexistence of the cavities and periodic corrugations on the transition region in the hackle zone. The elastic wave causes significant periodic elastic stress field permeating the glassy phase in the path of the oncoming

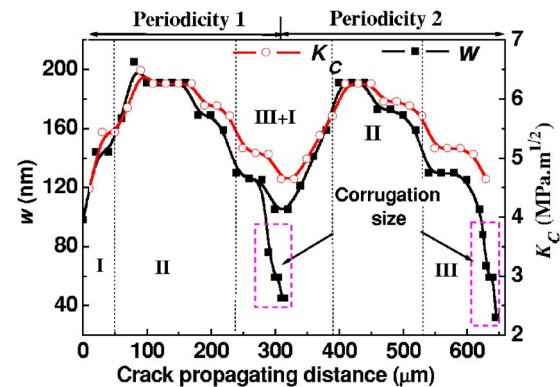


FIG. 3. (Color online) Size of damage cavities and toughness as functions of crack propagating periodic length. Regions I, II, and III correspond to the river-pattern, mist, and hackle zones, respectively.

crack, which results in directional preference of cavities.<sup>23</sup> Since we used the striplike samples ( $\sim 25 \mu\text{m}$  in thickness), the boundary of the strip should seriously affect the crack propagation because a part of elastic waves generated from the fast running crack front will be reflected and bring out a mode III perturbation and influence the fracture surface.<sup>4,14</sup> This perturbation is a possible reason resulting in the swirling pattern presenting on the hackle zone. The SEM observations indicate that the periodic corrugations seem to be the self-assembly of the cavities when their size reaches a critical value. We suggest that, based on the observations, a rotation stress field resulted from the twisted hackle pattern surface is seriously influenced by the elastic wave reflected from the boundary. Thus, a complicated directional stress field is formed, which reduces the local stress intensity factor, further decreasing the size of the damage cavity and increasing the density of cavities. A critical density of cavities is required because the self-assembly of cavities needs them to be close enough so that they are within each other's elastic influence range.<sup>18,23-25</sup> Therefore, the periodic corrugation pattern is formed on the surface of the hackle zone. Furthermore, the impaction of the elastic waves reflected from the boundary on the twisted crack front can modulate the periodicity of the stress field. It can be expected that if the wavelength of the modulated stress field is of same order as the characteristic size of plastic process zones, the periodic corrugation pattern can be formed as shown in Fig. 1(d).

In summary, the crack propagation process of the brittle  $\text{Fe}_{73.5}\text{Cu}_1\text{Nb}_3\text{Si}_{13.5}\text{B}_9$  glassy ribbon generates the periodic fractography consisting of river-pattern, mist, and hackle zones presenting on the fracture surface. This periodic morphology reflects the size changing in plastic process zone of crack tip, which suggests that the crack propagation is dominated by the wavy stress intensity change. The formation of nanoscale damage cavity structures is a common characteristic morphology in all the different zones. The nanoscale swirling periodic corrugation patterns formed by the self-assembly of the cavities are ascribed to the coimpact of the

rotated stress field due to the twisted hackle pattern surface and the reflected elastic waves interfering with the plastic process zone on the crack front.

Financial support from the NSFC (Nos. 50321101, 50371098, and 50371097) is acknowledged.

- <sup>1</sup>L. B. Freund, *Dynamic Fracture Mechanics* (Cambridge University Press, Cambridge, 1990).
- <sup>2</sup>B. N. Cox, H. Gao, D. Gross, and D. Rittel, *J. Mech. Phys. Solids* **53**, 565 (2005).
- <sup>3</sup>J. Fineberg and M. Marder, *Phys. Rep.* **313**, 1 (1999).
- <sup>4</sup>D. Bonamy and K. Ravi-Chandar, *Int. J. Fract.* **134**, 1 (2005).
- <sup>5</sup>B. Lawn, *Fracture of Brittle Solids*, 2nd ed. (Cambridge University Press, Cambridge, 1993).
- <sup>6</sup>E. Sharon and J. Fineberg, *Nature (London)* **397**, 333 (1999).
- <sup>7</sup>R. D. Deegan, P. J. Petersan, M. Marder, and H. L. Swinney, *Phys. Rev. Lett.* **88**, 014304 (2002).
- <sup>8</sup>A. Yuse and M. Sano, *Nature (London)* **362**, 329 (1993).
- <sup>9</sup>W. G. Kanuss and K. Ravi-Chandar, *Int. J. Fract.* **27**, 127 (1985).
- <sup>10</sup>E. K. Beauchamp, *J. Am. Ceram. Soc.* **78**, 689 (1995).
- <sup>11</sup>J. E. Field, *Contemp. Phys.* **12**, 1 (1971).
- <sup>12</sup>A. M. Fitzgerald, T. W. Kenny, and R. H. Dauskardt, *Exp. Mech.* **43**, 317 (2003).
- <sup>13</sup>T. A. Michalske and V. D. Frechette, *Int. J. Fract.* **17**, 251 (1981).
- <sup>14</sup>D. Bonamy and K. Ravi-Chandar, *Phys. Rev. Lett.* **93**, 099602 (2004).
- <sup>15</sup>E. Sharon, G. Cohen, and J. Fineberg, *Phys. Rev. Lett.* **88**, 085503 (2002).
- <sup>16</sup>E. Bouchaud, J. P. Bouchaud, D. S. Fisher, S. Ramanathan, and J. R. Rice, *J. Mech. Phys. Solids* **50**, 1703 (2002).
- <sup>17</sup>N. H. Tran and R. N. Lamb, *Chem. Phys. Lett.* **391**, 385 (2004).
- <sup>18</sup>J. J. Lewandowski, W. H. Wang, and A. L. Greer, *Philos. Mag. Lett.* **85**, 77 (2005); X. K. Xi, D. Q. Zhao, M. X. Pan, W. H. Wang, Y. Wu, and J. J. Lewandowski, *Phys. Rev. Lett.* **94**, 125510 (2005).
- <sup>19</sup>F. Spaepen, *Acta Metall.* **25**, 407 (1977); A. S. Argon, *ibid.* **27**, 47 (1979); M. F. Ashby and A. L. Greer, *Scr. Mater.* **54**, 321 (2006); K. M. Flores and R. H. Dauskardt, *ibid.* **41**, 937 (1999).
- <sup>20</sup>B. Yang, M. L. Morrison, P. K. Liaw, R. A. Buchanan, G. Wang, C. T. Liu, and M. Denda, *Appl. Phys. Lett.* **86**, 141904 (2005); J. J. Lewandowski and A. L. Greer, *Nat. Mater.* **5**, 15 (2006).
- <sup>21</sup>A. S. Argon and M. Salama, *Mater. Sci. Eng.* **23**, 219 (1976).
- <sup>22</sup>E. A. Brener and V. I. Marchenko, *Phys. Rev. Lett.* **81**, 5141 (1998).
- <sup>23</sup>X. K. Xi, Doctoral thesis, Institute of Physics, Chinese Academy of Sciences, 2005.
- <sup>24</sup>R. P. Kusy and D. T. Turner, *Polymer* **18**, 391 (1977).
- <sup>25</sup>K. Ravi-Chandar and B. Yang, *J. Mech. Phys. Solids* **45**, 535 (1997).